PNAS RESEARCH ARTICLE | MICROBIOLOGY

Extensive heterozygosity and genetic exchange among natural populations of *Leishmania* species

Eliza V. C. Alves-Ferreira[a,1], Mourad Barhoumi[a,b,1], Tiago R. Ferreira[c], Matthew W. Brown[d], Petr Volf[e], Yusr Saadi-BenAoun[b], Immen Khammari[f], Ihcen Kherachi[g], Akila Fathallah Mili[f], Zoubir Harrat[g,2], Ikram Guizani[b], David L. Sacks[c], Julius Lukeš[h,i,3], and Michael E. Grigg[a,3]

Affiliations are included on p. 9.

Contributed by Julius Lukeš; received January 6, 2026; accepted March 21, 2026; reviewed by Tom Beneke and Luigi Gradoni

Genetic hybridization within the genus *Leishmania* has been demonstrated experimentally, but the extent to which this occurs naturally among circulating populations remains enigmatic. The current consensus is that natural populations undergo preponderant clonal evolution, presumably expanding by asexual replication. To investigate the extent to which inter- and intraspecific genetic exchange has impacted *Leishmania* population genetics, a pan-genus multilocus typing method composed of 27 linked and unlinked genetic markers under purifying, neutral, or positive selection was developed and applied against 254 *Leishmania* isolates assigned to 11 species, the majority (n = 142) of which had been previously speciated using isoenzyme or DNA sequence typing methodologies. Phylogenetic trees and network analyses identified high levels of heterozygosity and allelic diversity across diverse geographic regions, challenging conventional species designations. Notably, approximately 72% of isolates displayed genetic hybridization, both inter- and intraspecific, resulting in hybrids possessing heterozygous sequence blocks from distinct parental ancestries. Whole-genome sequencing analyses performed on 24 isolates validated the hybridization findings. These results underscore a higher degree of outbreeding within the "Old World" *Leishmania* populations than previously envisaged. Understanding the genetic dynamics and role of hybridization within the population genetics of *Leishmania* will provide crucial insight for the design of targeted interventions that mitigate the spread of the debilitating tropical diseases caused by these parasites.

Leishmania | genetic exchange | whole-genome analysis | population genetics | MLST

Significance

Hybridization is increasingly recognized as a powerful evolutionary force, yet the extent to which it impacts the population genetics of *Leishmania* remains enigmatic. Previous work suggested that *Leishmania* propagation is predominantly by clonal expansion. However, a pan-genus multilocus typing scheme that we developed to select isolates for whole-genome sequencing from over 250 broadly distributed "Old World" isolates showed that genetic exchange is pervasive across major human-infective species. More than 70% of the isolates showed mosaic ancestry presumably derived from inter- and intraspecific hybridization. Our data reveal a highly reticulated population structure that current species definitions fail to capture. Recognizing the central role of hybridization has significant implications for the taxonomy, fitness, transmission, and the emergence of pathogenic and/or drug-resistant clones.

Leishmaniases are neglected tropical diseases caused by kinetoplastid parasites belonging to the genus *Leishmania* that are naturally transmitted by infected sand fly bites (1). Having a global distribution, leishmaniases correspond to a wide spectrum of clinical syndromes, including tegumentary and visceral diseases, that range from asymptomatic to severe. Current estimates indicate that over 12 million people are affected globally, with 1 billion people at risk of contracting various forms of the disease (2–4). Over twenty widely distributed species of *Leishmania* are pathogenic to people, several are classified as zoonoses (5) and 4 species in particular (*L. major, L. donovani, L. infantum,* and *L. tropica*) are responsible for transmitting the majority of clinical cases in the Old World (2).

The degree to which natural populations of these parasitic protists expand sexually versus asexually in nature is central to understanding disease potential, transmission dynamics, and their population genetic structure. Such information is crucial if we are to develop targeted strategies to reduce the burden of disease. Genetic hybridization is an important trait in the evolution and acquisition of virulence potential among a wide-range of unicellular eukaryotic pathogens, including fungi (*Cryptococcus* spp.) and protists (*Toxoplasma* and *Plasmodium*) (6–8). Whether kinetoplastids (*Leishmania* spp., *Trypanosoma* spp.) with hitherto cryptic sexual cycles utilize genetic exchange to produce new strains capable of causing disease has not been systematically assessed. Previous work suggested that the predominant mode of their propagation in nature is by asexual (or clonal) expansion, largely the result of finding widespread identical genotypes in high linkage disequilibrium without significant heterozygosity when only limited genetic markers were applied that were selected to be species-specific (9). Paradoxically, many reports of hybrid genotypes have identified a high occurrence of inter- and intraspecific hybridization among natural populations (10), including field studies that investigated vector-isolated *L. infantum* strains from southeastern Türkiye and cutaneous *L. donovani* clinical isolates from both Ethiopia and Sri Lanka at whole genome sequence (WGS) resolution (11–13). Coupled with laboratory crosses that demonstrate no significant genetic barriers, constraints, and/or limits on inter- and intraspecific hybridization, a reevaluation of the current population

The authors declare no competing interest.

[1]E.V.C.A.-F. and M.B. contributed equally to this work.

[2]Present address: Algerian Academy of Sciences and Technologies, Algiers 16015, Algeria.

[3]To whom correspondence may be addressed. Email: jula@paru.cas.cz or griggm@niaid.nih.gov.

This article contains supporting information online at https://www.pnas.org/lookup/suppl/doi:10.1073/pnas.2537999123/-/DCSupplemental.

Published April 17, 2026.

genetic structure was overdue to investigate the extent to which naturally circulating parasites utilize genetic hybridization to diversify or generate new biological potential that benefit transmission (14–17).

This study developed an innovative, pan-*Leishmania* multilocus sequence typing (MLST) scheme that is unbiased to determine the true rates of linkage disequilibrium, heterozygosity, and whether genetic exchange, including inter- and intraspecies recombination, has impacted the natural population genetic structure within the genus *Leishmania*. This methodology was applied against 254 *Leishmania* isolates, most of which had been previously typed by either multilocus enzyme electrophoresis (MLEE) or MLST methodologies and assigned both a Montpellier (MON) type and species designation. Our results identified unexpectedly high levels of both heterozygosity and allelic diversity across a wide geography and identified natural cross-species and intraspecific hybrids among naturally circulating strains within the "Old World" *Leishmania* species, including the most frequent ones, namely *L. infantum*, *L. major*, *L. tropica, L. donovani,* and *L. archibaldi* [now considered synonymous with *L. donovani* (18)]. Approximately 72% of the isolates examined within these 5 species were genetic hybrids that possessed either or both intra- and interspecific introgression and within the regions of heterozygosity it was possible to phase two distinct parental ancestries. In addition, we performed Whole Genome Sequencing (WGS) on 24 isolates distributed across these *Leishmania* species. The analyses revealed extensive inter- and intraspecific hybridization with patchy heterozygosity and phased haplotypes indicating recombinant origins rather than random allele distributions caused by drift. This mosaic inheritance was observed across species known to cause cutaneous disease (*L. major* and *L. tropica*), as well as those within the *L. donovani* complex that predominantly cause visceral disease (a related group of 3 species including *L. donovani, L. infantum,* and *L. archibaldi*), demonstrating ongoing genetic diversity and hybridization. Our results poignantly suggest that current species designations within the genus *Leishmania* fail to fully explain the extent to which outbreeding and/or inbreeding (between similar, yet distinct isolates within a species) is occurring among natural populations circulating in the Old World.

Results

***Pan-Leishmania* MLST Schematic Identifies Unexpected Levels of Allelic Diversity and Heterozygosity.** The majority of current genetic markers employed to assess population genetic structure in *Leishmania* are species-specific. We developed 24 nuclear and 3 mitochondrial (= kinetoplast DNA [kDNA]) linked and unlinked genetic markers, representing 14.4 kb of nucleotide sequence, to detect the alleles present for each marker across 11 examined *Leishmania* species. This unbiased, pan-genus *Leishmania* typing method was applied against 254 isolates of predominantly Old World species, the majority (n = 142) of which had been previously speciated using isoenzyme or DNA sequence typing methodologies (Fig. 1*A* and *SI Appendix*, Table S1). The pan-Leish typing markers produced a genetic fingerprint across 17 chromosomes and the kDNA maxicircle, specifically amplifying the alleles present within the genus *Leishmania*, including the lizard-infecting *L. tarentolae*, but not related kinetoplastids, represented by *Trypanosoma cruzi* (Fig. 1*B* and *C*). The pan-Leish typing markers were under purifying, neutral, or positive selection and possessed an excess of heterozygosity. Specifically, 1023 heterozygous sites were present across the 27 loci examined, obtaining an average of 7.1% polymorphism across the human-infective *Leishmania* spp. analyzed (*SI Appendix*, Table S2). The ratio of nonsynonymous to synonymous substitutions, or calculated dN/dS probabilities, identified 5 loci under purifying selection ($P < 0.05$), whereas 19 loci were under neutral ($P > 0.05$ to 1.0) and 1 under positive selection ($P > 1.0$) (*SI Appendix*, Table S2). The level of heterozygosity varied by species, with higher levels detected in *L. tropica* (49.7%), *L. donovani* (19.6%), and *L. infantum* (2.34%), with *L. major* being predominantly homozygous (0.18%).

Phylogenetic Incongruence and Heterozygosity Are Compatible With Genetic Exchange. The clonal theory for the parasitic protists presupposes that genetic exchange is infrequent and insufficient to break preponderant clonal evolution (19). Fixed heterozygosity, a perceived lack of recombinant genotypes, and the existence of widespread identical genotypes across typing markers in linkage disequilibrium is thought to support an asexual expansion model for Old World *Leishmania* spp. (20). Specifically, that variation within a MON type is rather explained by genetic drift, through the accumulation of private SNPs, that result in increased heterozygosity, consistent with the Meselson effect for diploid organisms which replicate exclusively asexually and accumulate mutations over time that cause two homologous chromosomes to diverge, as described for *Trypanosoma brucei gambiense* (21). To determine if the level of heterozygosity identified supported an asexual expansion model, we generated alignments and produced phased phylogenetic trees for each of the 27 markers to visualize heterozygosity and identify the degree to which it was random or had occurred in blocks, the result of inheriting two parental haplotypes consistent with genetic exchange across the 254 isolates (Fig. 1*D* and Dataset S1).

Locus-specific trees identified only a limited number of allelic types, consistent with a nonrandom inheritance of heterozygosity. At every locus, only between 5 to 15 allelic types were resolved across all species investigated. To better illustrate this genetic diversity in a distance-based framework, we produced haplotype network diagrams for all 27 markers. For 5 markers (5_180; 9_740; 14_nh2; 27_2335; 35_2160) each allele for the main species studied (*L. infantum, L. donovani, L. major,* and *L. tropica*) was represented by a circle of a particular color hue, and circle size was dependent on the frequency of the allele in the population (*SI Appendix*, Fig. S1).

The network diagrams established that *L. major* (red) had one dominant allele with only 1 or 2 other alleles that were less divergent compared to *L. tropica* (orange), which had between 3 to 6 alleles that were equally distributed across the isolates and more divergent. Within the *L. donovani* complex, both major and minor alleles (4 to 10 depending on the marker) segregated either as *L. donovani* (blue) or *L. infantum* (green) alleles. However, at every locus, some *L. donovani* speciated isolates possessed *L. infantum* alleles (blue in green), some *L. infantum* speciated isolates possessed *L. donovani* alleles (green in blue), and the 2 *L. archibaldi* isolates had a combination of blue and green alleles. When integrated across all markers, the data indicated a high level of inter- and intraspecific hybridization events had occurred within the genus (*SI Appendix*, Fig. S1). To distinguish between alleles having undergone minor mutational drift from those that had evolved independently as distinct genetic outgroups, phylogenetic trees were generated with 1,000 bootstrap replicates run for each tree, and supported nodes above 50% were indicated at each marker. The majority of allelic types had significant bootstrap support suggesting that the limited number of alleles present had evolved independently and that they appeared to segregate independently across the isolates. For those isolates where heterozygosity existed, biallelic positions

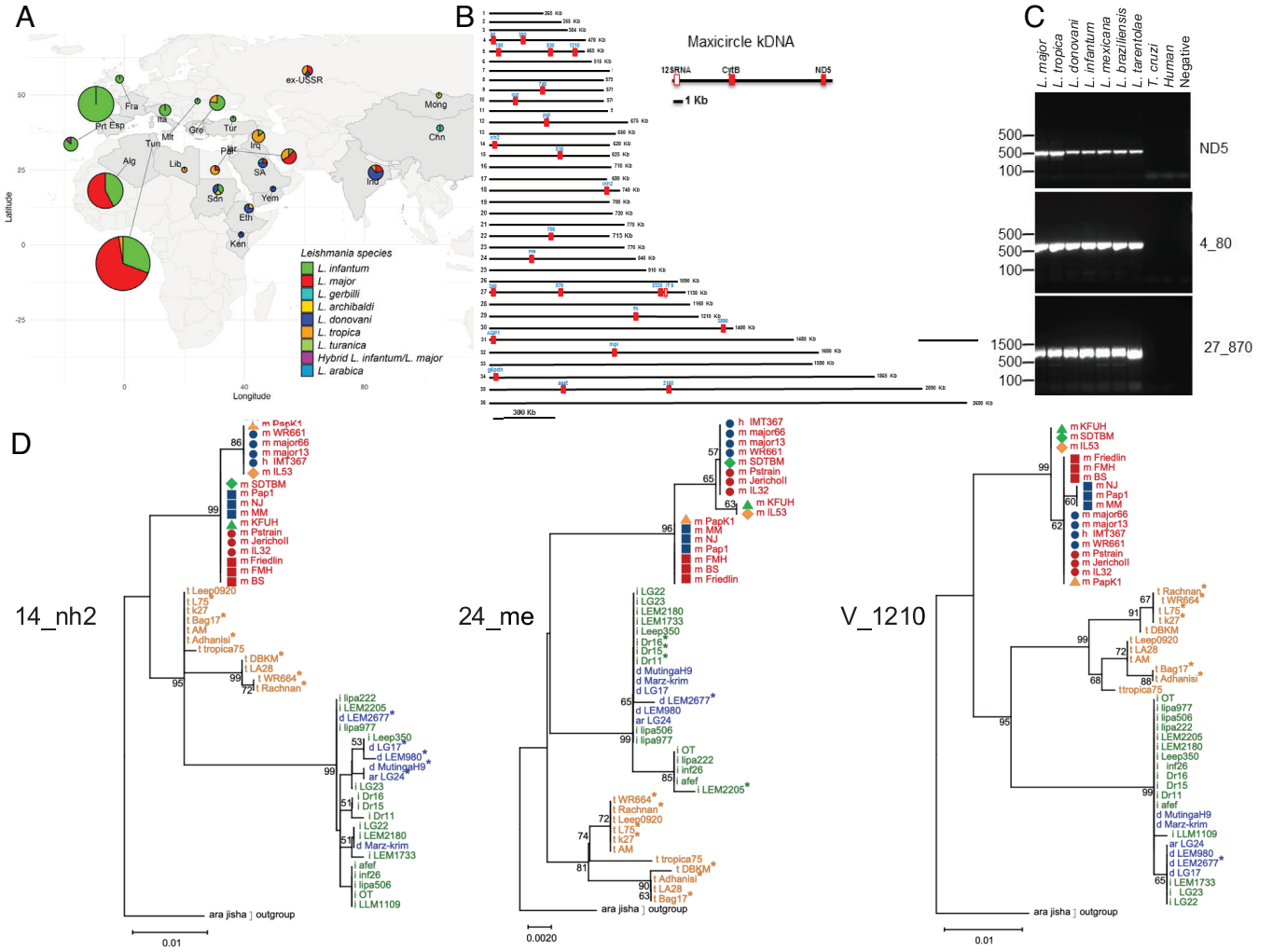

Fig. 1. Geographical distribution of *Leishmania* isolates and chromosomal markers for MLST investigation. (*A*) Geographical distribution of 254 *Leishmania* isolates used in this study. Each color corresponds to the species previously typed. The numerical value within each circle shows the number of isolates studied from each country. (*B*) Chromosome positions of 27 nuclear and mitochondrial linked and unlinked pan-*Leishmania* markers used for MLST investigation. (*C*) The agarose gel illustrates a pan-genus PCR amplification for 5 of endogenous markers. (*D*) Neighbor joining phylogenetic trees for a subset of *Leishmania* isolates using the markers 5_120, 24_me, and 14_nh2. The color of each allele represents the assigned species for each isolate based on MON or genetic typing, with green indicating *L. infantum*, blue for *L. donovani*, red for *L. major*, and orange for *L. tropica*. Incongruences were identified across all loci between the allele identified versus the species designation within the *L. donovani* complex. Isolates demonstrating heterozygosity at each locus are marked with an asterisk in each phylogenetic tree. For each heterozygous position, only the alternate allele was added to the tree. Heterozygosity was observed in all species at all loci except for a few *L. major* isolates. Bootstrap values >50% were calculated and are displayed at the nodes, with asterisks denoting the positions of heterozygotes.

were readily phased into parental haplotypes that had already been described across the total number of isolates sequenced. The relative lack of private SNPs was quite remarkable, unexpected and supported a meiotic origin to explain the extant heterozygosity—that disomic inheritance of limited allelic types was observed at every locus. Furthermore, phylogenetic incongruence in the strain topology between markers was observed, extensively for *L. tropica* and *L. donovani,* but also for *L. major*. For example, for 12 *L. major* isolates (IL53, KFUH, SDTBM, Papk1, Pstrain, JerichoII, WR661, WR662, major13, major16, BS and FMH) across just 3 markers, segregation of homozygous allelic types produced 7 haplotypes (Fig. 1*D*). Isolates belonging to each of the 7 haplotypes were annotated by a different geometric shape and color (Fig. 1*D*). Genetic hybridization is the most parsimonious explanation to describe the inheritance of the alleles across these isolates. Additionally, within the *L. donovani* complex, at the same 3 markers, multiple examples of isolates with MON-types belonging to the *L. donovani* species (in blue) resolved with *L. infantum* alleles, and vice versa, suggesting that the admixtures of green and blue across the markers were due to recombination (Fig. 1*D*). The possibility of mixed infection(s) was ruled out for these interspecific hybrids, since all sequenced isolates possessed only one species-specific allelic type at the ND5, CytB, and 12S markers in the kDNA maxicircle, which is uniparentally inherited (17).

Previous work applying microsatellite markers on 106 isolates within the MON-1 type suggested the possibility of recombination to explain both pathology and phenotypic diversity within MON-1 (22). Our study investigated 49 MON-1 assigned isolates and resolved 22 haplotypes using robust gene-specific markers less prone to the rapid evolution and back mutations that occur with microsatellite markers. Expanding our analysis to other MON types, including the *L. infantum* MON-24 type, resolved 7 haplotypes within just 8 isolates, and for the *L. major* MON-25 type, 5 haplotypes were resolved across 19 isolates, again supporting a meiotic origin for many isolates within each MON type (*SI Appendix*, Table S3).

High Incidence of Recombinants and Interspecies Hybrids. We next generated an allelic inheritance plot to more precisely integrate the number of alleles for every marker present within

each speciated isolate across all 254 samples (Fig. 2). Isolates were arrayed geographically, with each column representing a genetic marker and the color at each marker (blue, green, red, orange) reflected ancestry. Hues within a color group represent different alleles. It was possible to phase the alleles for all heterozygous positions, and for those markers with 2 alleles, these were indicated by 2 color hue blocks at the marker. The allele inheritance plot established that *L. major* possessed a low level of intraspecific heterozygosity that partitioned largely geographically. The inheritance of 2 separate alleles at the nuclear markers on chromosomes 4, 29, 31, and 34 was particularly evident. Of the 106 isolates that had been previously speciated as *L. major*, 50 (47%) had a signature of intraspecific hybridization using the 27 marker fingerprint. All 18 *L. donovani* and 21 *L. tropica* isolates were identified as hybrids based on the presence of phased parental alleles at ≥2 independent loci as defined in Materials and Methods. All *L. donovani* isolates, including the reference genome isolate LV9, were interspecific hybrids with *L. infantum*, whereas *L. tropica* isolates were exclusively intraspecific hybrids and possessed higher levels of heterozygosity. Of the 78 MON-typed

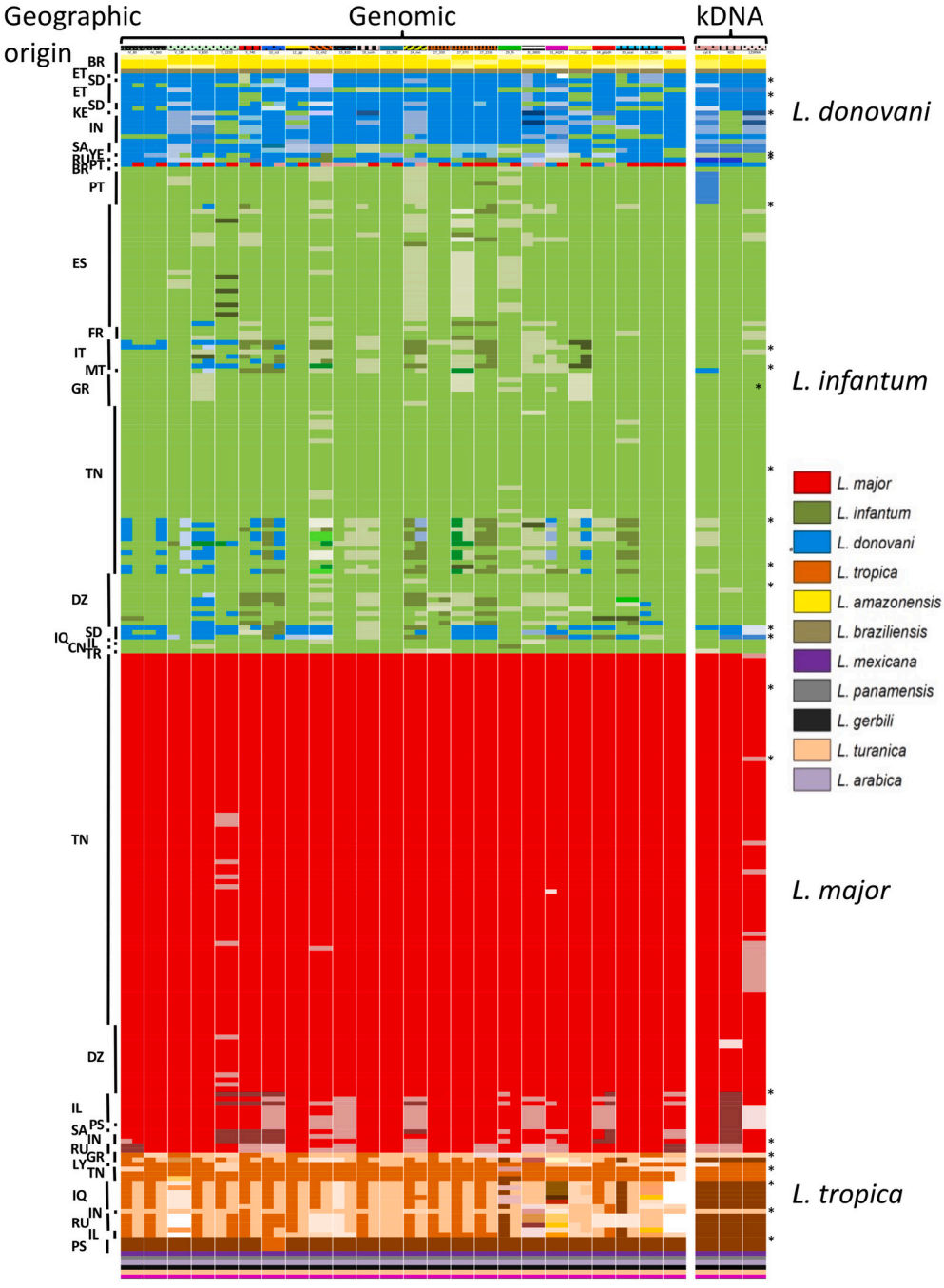

Fig. 2. Allele Inheritance plot for 254 *Leishmania* isolates at 27 genetic markers shows that genetic hybridization is extant in natural isolates. The plot highlights the genetic variation for each isolate. Each column represents a genetic marker while each row an isolate. Markers are listed in *SI Appendix*, Table S2. Samples are organized based on their geographic origin and MON-typed classification, with isolate information provided in *SI Appendix*, Table S1. For each marker, at least 1 allele was identified for each species, and at loci when two alleles were resolved, distinct color hues were used to illustrate the inheritance patterns of both alleles across the examined loci. Specifically, two color hues were used for markers exhibiting heterozygosity, that represented the two alleles present and their origin.

L. infantum isolates, a single haplotype was observed in 12 (15%) isolates, whereas 66 (85%) were identified as hybrids, 40 (51%) and 26 (33%) of which were intra- and interspecific, respectively. Of note, interspecific hybrids clustered geographically. The allele inheritance plot supported a greater degree of hybridization in the generation of these naturally propagated, mosaic clones than previously described. While our results do not preclude asexual (or clonal) expansion as a primary mode of transmission, the relative dearth of private SNPs does suggest that sexual reproduction is occurring at levels not previously envisaged.

WGS Analysis Supports Ongoing Inter- and Intraspecific Hybridization Among Old World Isolates. We performed WGS on 24 isolates from 5 Old World species selected from the MLST data that possessed either no or various levels of inter- or intraspecific variation to more precisely determine genetic diversity, heterozygosity, ploidy, and SNP variation across each genome (Fig. 3*A* and *SI Appendix*, Fig. S2*A*). Mean read depth genome-wide was 35.2× (ranging from 30 to 200× coverage), and each isolate was mapped to their closest related reference genome: *L. tropica* (L590, Israel), *L. major* (Friedlin, Israel), *L. infantum* (JPCM5, Spain), or *L. donovani* (LV9, Sudan) (*SI Appendix*, Table S4). Ploidy analysis established that the majority of samples were diploid, except at chromosome 31, as is commonly observed. Six isolates displayed a patchwork of polysomy at either 1 or 2 of chromosomes 2, 4, 8, 23, 26, and 33 (*SI Appendix*, Fig. S2*B*). A neighbor-joining network analysis plotted using homozygous SNPs established that the reference genomes of *L. major, L, donovani,* and *L. tropica* were genetically quite distinct from the sequenced samples, whereas the majority of *L. infantum* isolates shared a close ancestry with the JPCM5 reference (Fig. 3*B*). Both *L. archibaldi* isolates (LG24 and GEBREI) possessed alleles at the kDNA maxicircle that claded with *L. donovani,* yet the LG24 genome clustered more closely with *L. infantum,* supporting an *L. donovani* x *L. infantum* hybrid origin to describe at least 2 isolates previously designated as *L. archibaldi.* Further, reticulations in the network tree identified the *L. donovani* reference genome LV9 as recombinant, and a hybrid origin for the majority of *L. tropica* genomes (Fig. 3*B*; *Inset*).

Patchy Heterozygosity and Haplotype Phasing Identifies Extant Mosaicism Among Sequenced Genomes. To evaluate SNP variation, all genomes were mapped to the reference genome determined empirically to be phylogenetically closest, which was not necessarily the genome of the MON-typed species designation. In this regard, *L. archibaldi* isolate LG24 and *L. infantum* isolates LG23 and Leep350 were mapped against LV9, whereas *L. donovani* isolate Marz-krim was mapped against JPCM5 (*SI Appendix*, Table S4). All 4 *L. major* isolates were genetically distinct from the reference Friedlin genome, with ~44,000-49,000 homozygous SNPs uniformly distributed across their genomes (Fig. 4). Isolates BS and FMH possessed very limited heterozygous (*He*) SNPs (~1,400 each) but a high number of homozygous (*Ho*) SNPs, whereas IL24 and SDTBM had both high numbers of *Ho* and *He* SNPs (*He* frequency was ~22%). However, the high level of *Ho* SNPs distinct from Friedlin was numerically greater than the patchy blocks of *He* SNPs, so these lines were not considered full genome hybrids and were colored as a single ancestry in the Circos plots generated by the PAINT software (Fig. 4*A*).

In contrast, locus-specific trees for SDTBM, as well as many other *L. major* isolates including Papk1, Pstrain, Jericho II,

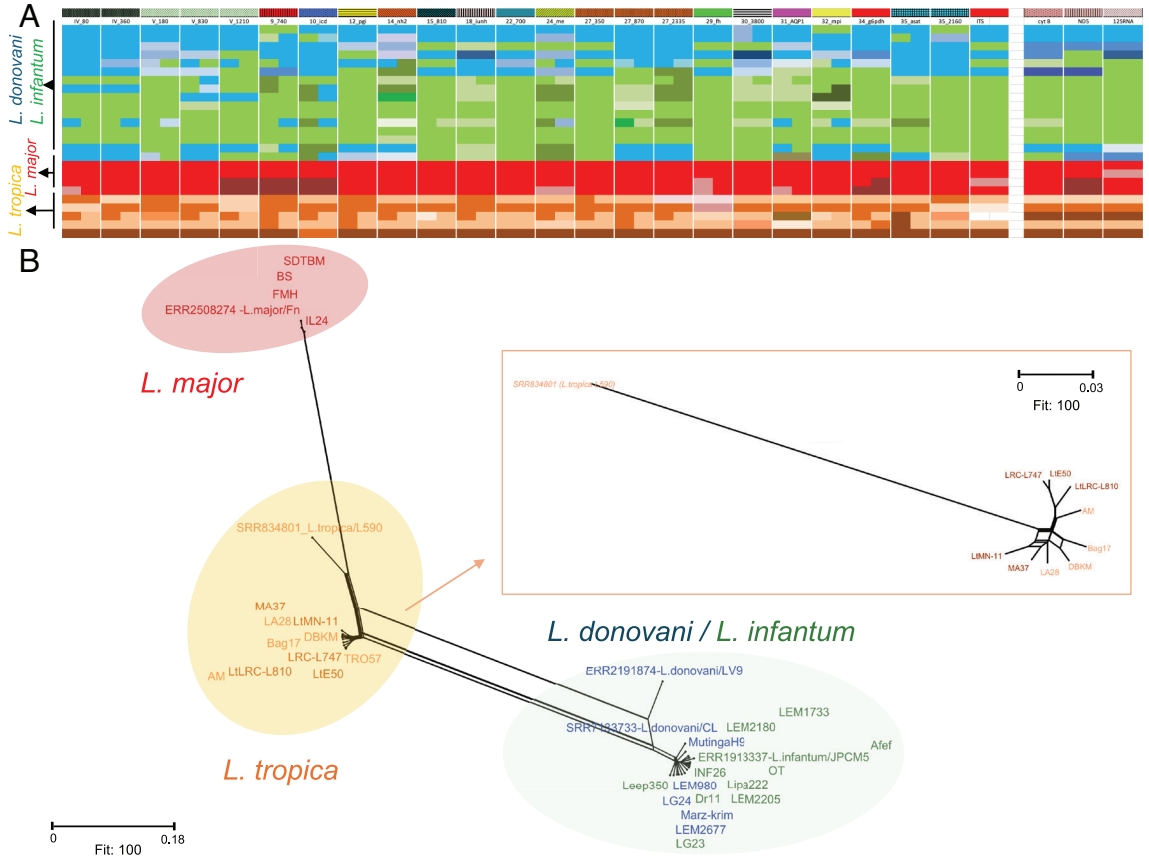

Fig. 3. Intraspecific whole-genome comparison of human isolates. (*A*) Allele inheritance plot for 24 isolates submitted to whole-genome sequencing (WGS). (*B*) Whole-genome phylogenetic network of clinical *Leishmania* spp. isolates based on 1,294,404 high-quality *Ho* SNPs.

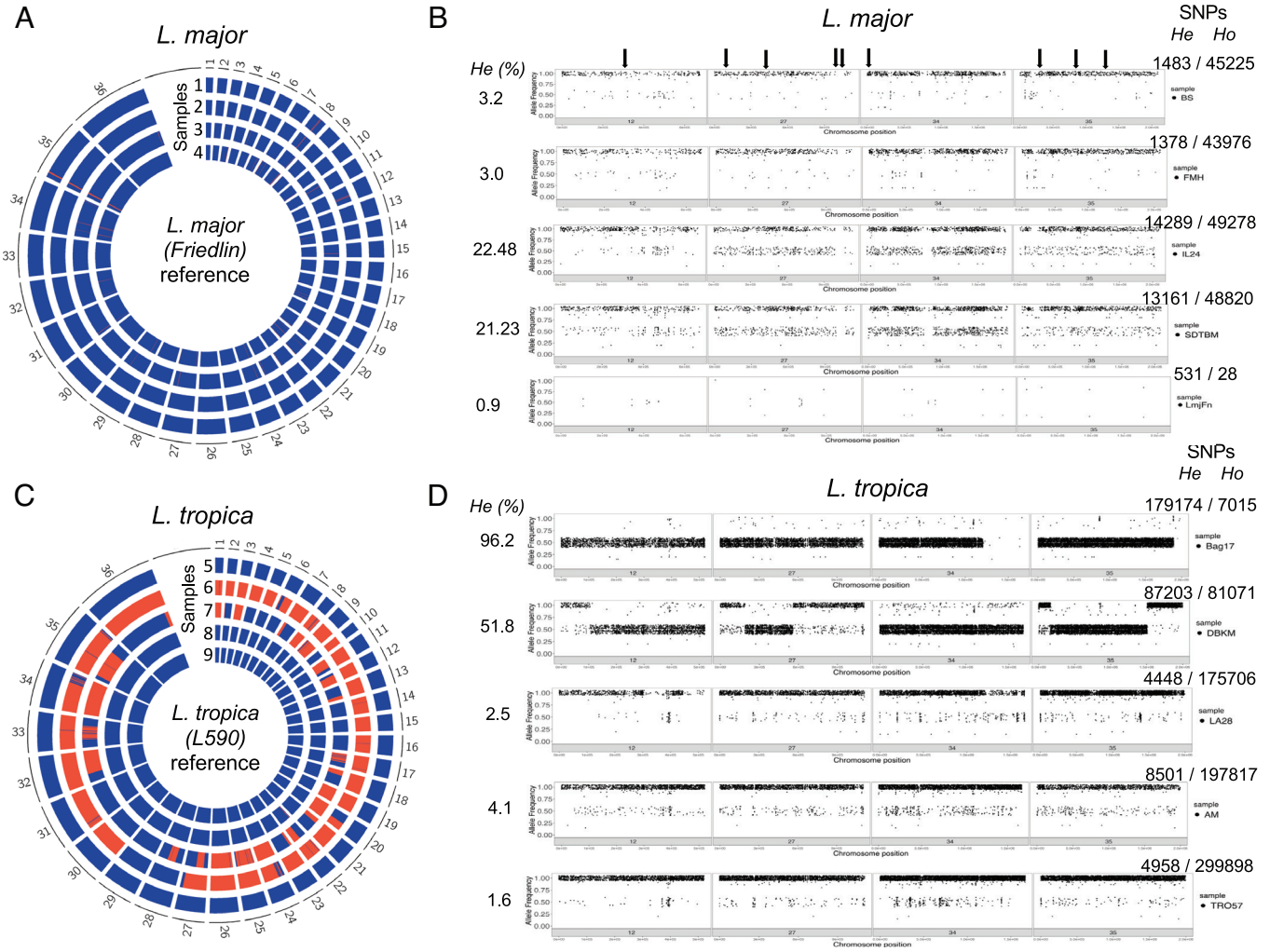

Fig. 4. Whole-genome analysis of *Leishmania* major and Leishmania tropica. (*A*) RCircos plot of *L. major* showing homozygous SNPs (blue) and heterozygous SNPs (red) across 36 chromosomes. (*B*) SNP density plots for selected chromosomes (12, 27, 34, and 35) of *L. major*. (*C*) RCircos plot of *L. tropica* showing homozygous SNPs (blue) and heterozygous SNPs (red) across 36 chromosomes. (*D*) SNP density plots for selected chromosomes (12, 27, 34, and 35) of *L. tropica*. Heterozygous SNPs were defined as having an allele frequency between 40% and 60%, whereas homozygous SNPs had a frequency ≥85% within a 5-kb window. Genomes were aligned to reference strains based on genetic typing: *L. major* Friedlin (*A* and *B*) and *L. tropica* L590 (*C* and *D*). *He*, heterozygous; *Ho*, homozygous. Arrows indicate the genomic positions of the nine MLST markers across the chromosomes shown.

WR661, WR662, KFUH, major13, and major66, possessed at some loci the dominant allele present across the population, but at other loci, the inherited allele was distinct and had evolved independently with strong bootstrap support (Fig. 1*C* and Dataset S1). This patchwork inheritance of dominant and alternate alleles that segregated across loci to produce a distinct haplotype supported a recombinant origin for SDTBM. Furthermore, it was possible to phase the majority of the blocks of *He* using the dominant allelic type as one parental haplotype, with the other belonging to one or other of the alternate *Ho* alleles identified across the 106 *L. major* isolates. In effect, across the population, it was always possible to identify two parental *Ho* haplotypes for each region of mixed ancestry, which supported genetic hybridization of a limited set of alleles to explain *He*, rather than genetic drift, which would produce a pattern of inherited SNPs according to the Meselson effect. It also revealed an inherent bias in the PAINT software—that mapping genomes against divergent reference genomes during SNP calling effectively masks the ability to resolve signatures of hybridization in genome-wide datasets that contain patchy heterozygosity.

Among the 5 *L. tropica* genomes sequenced, isolates Bag17 and DBKM possessed genome-wide levels of *He*, but also a patchwork of long runs of homozygosity (LROH) that were either *Ho* SNP-poor (both haplotypes were similar to reference L590) or *Ho* SNP-dense (both haplotypes were divergent from L590), consistent with outcrossing by full-genome hybridization. In the Circos plots denoting SNP inheritance patterns, discrete blocks of red (regions of *He* SNPs) switching with blocks of blue (regions of *Ho* SNPs) were readily resolved, with distinct crossover points (Fig. 4*C*). The remaining 3 isolates (LA28, AM, TRO57) possessed high levels of *Ho* SNPs (ranging from ~175,000 to 300,000) with limited *He* SNPs (Fig. 4*D*), but as with *L. major*, locus-specific trees identified a minimum of 3 and up to 7 allelic types across the loci examined that had been inherited to produce distinct haplotypes that supported a distinct recombinant origin for every isolate, in addition to the intraspecific inheritance of 2 allelic types at those loci with *He* SNPs present.

Finally, all isolates within the *L. donovani* complex, including *L. donovani, L. archibaldi,* and *L. infantum*, were mapped against either the *L. donovani* LV9, or *L. infantum* JPCM5 reference genomes (*SI Appendix*, Fig. S4). Only 2 isolates (LG23 and LG24) possessed a patchwork of *Ho* SNP blocks that were similar to LV9 (SNP-poor) or different (SNP-dense). All other isolates had high levels of *Ho* SNPs different from LV9, and where blocks of *He*

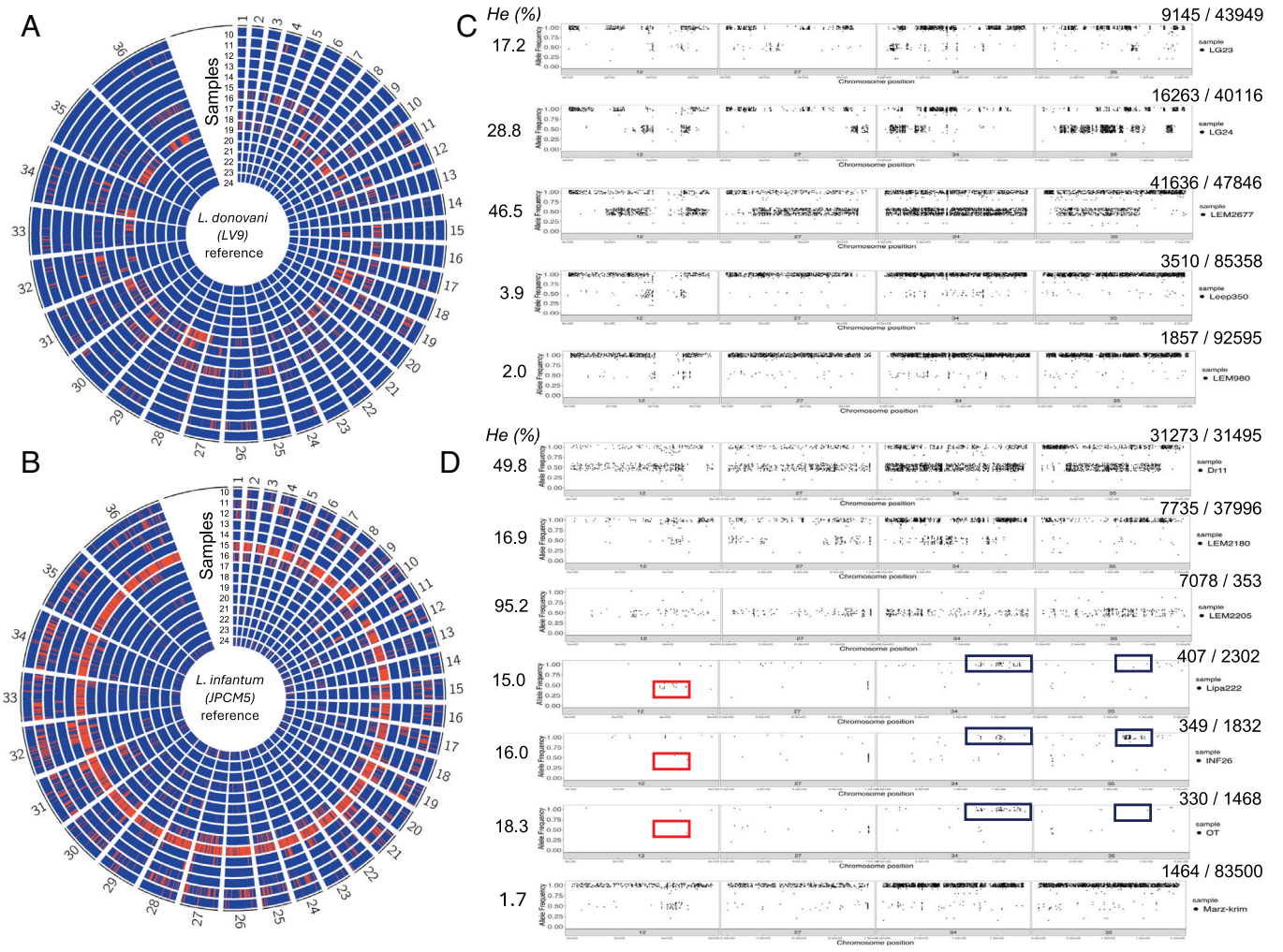

Fig. 5. Whole-genome analysis supports genetic hybridization in *L. donovani* and *L. infantum* isolates. The same genomes were mapped to *L. donovani* LV9 and *L. infantum* (JPCM5), revealing different numbers of SNPs depending on the reference genome used. (*A* and *B*) *Leishmania* RCircos plots of genomes mapped to *L. donovani* (*A*) and *L. infantum* (*B*) showing homozygous SNPs (blue) and heterozygous SNPs (red) across 36 chromosomes. (*C* and *D*) SNP density plots for selected chromosomes (12, 27, 34, and 35) of the isolates: mapped to *L. donovani* (*C*) and *L. infantum* (*D*), respectively. *He* = heterozygous; *Ho* = homozygous.

SNPs existed (Fig. 5*A*), both phased haplotypes were different from LV9. When the same isolates were mapped against JPCM5, the mosaicism within the genomes was more highly resolved, because the majority of isolates were either *Ho* SNP-dense (one or both parental haplotypes were different from JPCM5) or *Ho* SNP-poor, with both haplotypes similar to JPCM5, in which case, blocks of patchy heterozygosity were easily identified in the Circos plots (Fig. 5*B*). Whereas mapping to the closer reference genome reduced overall SNP counts, the block-like structure of *He* was conserved, arguing against a mapping artifact and supporting ancestry mosaicism rather than a simple reference mismatch. Isolate Dr11 was identified as a full genome hybrid, and in the few LROH stretches resolved, it was *Ho* SNP-dense, and different from JPCM5. Another full genome hybrid, LEM2205, had LROH stretches that were *Ho* SNP-poor, which was parsimonious with one of the parents having a genotype similar to JPCM5 (Fig. 5*D*). Other isolates, including Lipa222, INF26, OT, and Afef, were highly similar to JPCM5, but within each of them, it was possible to resolve patchy blocks of heterozygosity (see red box on chromosome 12 *for* Lipa222) (Fig. 5*D*) that were inherited differently across these isolates. Notably, in contrast to the long heterozygous tracts observed in *L. tropica,* the smaller and more fragmented blocks observed in these *L. donovani* isolates are compatible with either mitotic LOH processes or older hybridization events subsequently broken down through inbreeding or recombination. It was also possible to resolve blocks that were either *Ho* SNP poor (similar to JPCM5) or *Ho* SNP-rich (a haplotype related to but distinct from JPCM5) (Fig. 5*D*). Again, these were inherited differently as admixture blocks, supporting a genetic hybridization model (recombinant origin) rather than the Meselson effect typically associated with clonal expansion.

Discussion

Our comprehensive multilocus and whole-genome analyses have revealed that natural populations of Old World *Leishmania* spp. undergo more genetic hybridization and outcrossing than previously envisaged. The prevailing consensus is that these parasites replicate in nature predominantly asexually and that traditional species designations—defined *via* MLEE, MON typing, or species-specific MLST panels—were historically developed using species-specific markers that were biased toward detecting homozygosity rather than mosaicism. However, by developing and applying a pan-genus MLST schematic spanning 27 nuclear and kDNA markers to 254 isolates, we show that hybridization is pervasive across the genus. Approximately 72% of analyzed isolates had inter- or intraspecific hybrid ancestry, and for 24 deeply sequenced genomes, we show that mosaicism is the rule. These results cannot be explained by

genetic drift or strict asexual propagation. Further, despite the high degree of hybridization observed, the isolates largely retained their species designation, as evidenced by the uniparental inheritance of the single cytb kDNA allelic type, which for the vast majority of isolates, tracked with their respective species designations.

Across the genus, patterns of heterozygosity were not distributed randomly, nor were they consistent with a Meselson-type pattern expected under strictly clonal evolution. Instead, phased haplotypes showed that heterozygous blocks corresponded to limited, recurring parental allelic combinations consistent with a meiotic or meiotic-like genetic exchange previously documented in experimental crosses (14, 16, 17) and during inbreeding (23). Moreover, extensive phylogenetic incongruence across markers in *L. donovani*, *L. infantum*, *L. tropica*, and *L. major* demonstrated that recombination, not mutational drift, was the most parsimonious explanation for the number of haplotypes and allelic diversity observed. Using WGS, we further confirmed these conclusions by uncovering extensive patchworks of homozygous and heterozygous SNP blocks, reciprocal crossover breakpoints, and clear mosaic ancestries that were incompatible with long-term asexual propagation. While mosaic SNP blocks could theoretically arise through mitotic recombination or gene conversion, the absence of isolate-specific private SNP accumulation together with the recurrence of shared phased haplotypes across geographically distinct isolates argues against purely postclonal LOH processes and instead supports a hybrid ancestry. Further, the observed patchwork deficit in heterozygosity supports the premise that self-hybridization through the sand fly (inbreeding), which can cause the conversion of heterozygous genome blocks to reset to one or the other of the two parents, as responsible for the heterozygous haplotypes (23). While the outcome of this process could be interpreted to mirror that expected for an asexually propagated clone, the presence of "private" SNPs, a hallmark of the Meselson effect, was essentially absent within our sequence dataset. In fact, the near total absence of private SNPs rather supports ongoing sexual propagation, the frequency of which cannot be inferred, but its relevance for purging deleterious mutations that tend to accumulate during asexual reproduction may provide insight into the benefits conferred to *Leishmania* as they reproduce through the natural sand fly vector (23). Moreover, hybridization may enhance fitness within the sand fly vector, as demonstrated for the *L. infantum*/*L. major* hybrid (24).

Our results extend earlier studies identifying hybridization within the *L. donovani* complex that was originally thought to be rare (25). Our pan-genus MLST fingerprints and WGS datasets identified genetic mosaics as common. Cotton et al. (12) also reported mosaicism and hybridization in *L. donovani* circulating in Ethiopia and suggested that natural hybrids may contribute to phenotypic diversity and impact treatment efficacy. Rogers et al. (11) showed that the offspring of a single *L. donovani*/*L. infantum* hybrid was responsible for the establishment of a new focus of cutaneous leishmaniasis, which quickly spread through Southern Türkiye (26). Lypaczewski et al. (13) identified interspecific hybrids between *L. donovani* and *L. tropica* in Sri Lanka and suggested that these genetic hybrids possess new cutaneous disease phenotypes, with novel clinical outcomes. More recently, several studies using high-resolution population genomics showed that *L. infantum* circulating in the Mediterranean basin form recurrent hybrid lineages (11, 27), reinforcing the concept that genetic exchange is taxonomically widespread, and suggesting that may prove both evolutionarily and ecologically significant, and is not necessarily geographically restricted (26). Indeed, our data show that hybridization is not confined to isolated ecological niches or individual species complexes. Instead, it is a dominant feature within the genus *Leishmania.* The observation of extant interspecific events between *L. donovani* and *L. infantum*, the high levels of intraspecific recombination in *L. tropica*, and the occurrence of hybrid mosaicism within nearly half of the *L. major* isolates investigated has reinforced the concept that sexual propagation of *Leishmania* spp., a process that reshuffles their genomes and purges deleterious mutations, is ongoing, active, and pervasive. The fact that so many hybrids appear to be the products of independent mating events involving discreet parental lineages implies a striking frequency of sand fly coinfections. Whether the parents were obtained from a single feed on a coinfected host, or successive feeds on two different hosts is not known, although the current data demands that either or both scenarios are occurring with greater frequency than previously imagined.

Taken together, the detection of genetic hybridization across *L. major*, *L. tropica*, *L. infantum*, *L. archibaldi*, and *L. donovani* indicates that current species definitions underestimate the highly reticulated evolutionary landscape of this genus. Indeed, within the MON-1 zymodeme, 22 haplotypes were resolved, some of which resulted in visceral disease, while others caused only cutaneous lesions (*SI Appendix*, Table S3). Among 8 *L. infantum* MON-24 isolates, 7 recombinant haplotypes were resolved, all of which possessed at least one *L. donovani* allele across the markers investigated. Such hybridization has been shown to affect vector compatibility (10), while other studies suggest that it likewise impacts pathogenicity, host range, and drug susceptibility (28). This is not unlike other parasitic protists, including *Plasmodium* and *Toxoplasma* that utilize their sexual cycles to alter their biological potential (7, 29, 30). Recognizing this complexity is essential for accurate taxonomy, diagnostics, epidemiology, and the interpretation of clinical trials or drug efficacy studies where species identity is assumed to be defined and genetically stable. Indeed, the presence of pervasive mosaic genomes suggests that many isolates may not conform to a single taxonomic species.

In conclusion, our findings illuminate a far more dynamic and reticulated evolutionary landscape for these human pathogens than previously appreciated, underscoring the need to reconsider species boundaries and the potential role that sexual reproduction is playing to shape natural populations and the biology of *Leishmania*. Integrating hybridization into species definitions and evolutionary models will be critical for understanding how novel pathogenic lineages arise and spread, with direct implications for disease control in endemic regions.

Materials and Methods

Parasites. Total genomic DNA was extracted from 254 cryopreserved isolates using the DNeasy Blood and Tissue Kit (Qiagen), the majority classified as Old World *Leishmania* spp., collected from insect, animal, and human hosts between 1954 and 2011 in 25 countries. Most clinical samples have been typed *via* MON (n = 111) or MLST (in combination; n = 142) (*SI Appendix*, Table S1). For the remaining isolates, speciation was carried out by PCR amplification and RFLP analysis at the gp63 gene (31, 32) or within ITS1 (33).

Genetic Markers, DNA Extraction, MLST Genotyping, and dN/dS Calculation. A panel of 24 linked and unlinked pan-*Leishmania* nuclear and 3 kDNA markers were developed to cover 17 of the 36 chromosomes (4, 5, 9, 10, 12, 14, 15, 18, 22, 24, 27, 29, 30, 31, 32, 34, 35) at either housekeeping genes (25) or those with wide genomic distribution that were used in genetic crosses because they possessed polymorphisms that distinguish between *L. major* and *L. infantum* isolates (17), so the expectation was that they would be sufficiently polymorphic across the genus. Specifically, primers were designed in highly conserved regions within each target locus to ensure pan-genus amplification of predominantly human-infective species (i.e. *L. major*, *L. tropica*, *L. donovani*, *L. infantum*, and *L. braziliensis*) (*SI Appendix*, Table S5). Primers bracketed regions containing inter- and intraspecies polymorphisms in order to develop

a robust MLST methodology. To investigate whether typing loci were under neutral, purifying, or positive selection, an in-frame, codon-aligned multiple sequence alignment for each locus was converted to a PHYLIP file using a custom Python script. A maximum-likelihood gene tree was inferred from the PHYLIP alignment using IQ-TREE2 (34) with a nucleotide substitution model (GTR+Γ) and multithreading (e.g., -m GTR+G -st DNA -nt 2). The resulting Newick tree file (*.treefile) was used for downstream analyses. Nonsynonymous-to-synonymous substitution rates (ω = dN/dS) for each gene were produced using PAML v4 (codeml) (35) under the one-ratio "M0" model. Branch lengths were fixed (blength = 2). Codon analyses used seqtype = 1 (codons) and the F3×4 codon frequency model (CodonFreq = 2), with transition/transversion ratio (κ) and ω estimated from the data (fix_kappa = 0; fix_omega = 0). Two codeml runs were run per locus to assess the effect of ambiguous characters: i) ambiguity retained (cleandata = 0) and ii) ambiguous sites removed (cleandata = 1) (*SI Appendix*, Table S2). PCR was performed using Taq DNA polymerase (Sigma Aldrich D1806) in PCR buffer supplemented with 2 mM dNTPs and 10 mM $MgCl_2$, and 25 pM primers. The annealing temperature used was primer-specific, 55 °C or 58 °C. PCR amplicons were treated with ExoSAP-IT nuclease (Affymetrix, Product no. 78205) prior to DNA Sanger sequencing, which was performed at the NIAID Rocky Mountain Laboratories.

Phylogenetic Analysis. DNA sequences from each locus of the 254 isolates were aligned for each marker, chromatographs checked and trimmed using Lasergene SeqMan software, and each sequence was BLASTed to confirm the species identity. By ITS genotyping, the following species were resolved: 1 *L. arabica,* 2 *L. archibaldi,* 16 *L. donovani,* 103 *L. infantum,* 1 *L. gerbilli,* 106 *L. major,* 21 *L. tropica,* and 1 *L. turanica.* Edited sequences were aligned using the Clustal W2 algorithm and further processed for phylogenetic analysis. MSF files for each marker were imported into MEGA v6.06 to produce RaxML and Neighbor-joining (N-J) trees using a p-distance method, pairwise deletion for missing data, and 1,000 bootstrap support (36). Consensus trees were rooted using the outgroup allele from either *L. tarentolae* or *L. arabica*. Bootstrap support >50% was used to indicate a distinct allelic type. A Nexus file for each marker was imported into SplitsTree 4 v4.13.1 and NetworkNet analysis was run using default settings (37). Network diagrams for each locus were constructed using the TCS v1.21 software to calculate the frequency and generate a parsimonious network estimate that visualizes the genetic distance and relationship among alleles within a population when allelic diversity is low and recombination is possible. Biallelic heterozygous SNPs were assigned whenever overlapping peaks of the same height were observed in the DNA sequence electropherogram. Heterozygous SNPs were labeled with the IUPAC nomenclature for ambiguous base calls (K = G or T; M = A or C; R = A or G; Y = C or T; S = C or G; W = A or T). The gametic phase (or the haplotype sequence possessed by each of the two parental alleles represented within the diploid organism sequenced) for each of the heterozygous markers was determined based on the occurrence of a homozygous parental allele present in the other isolates examined. An isolate was classified as a hybrid if it possessed phased alleles at ≥2 independent nuclear loci that clustered phylogenetically with distinct parental haplotypes identified elsewhere in the population dataset. This criterion was used to distinguish hybrid ancestry from single locus heterozygosity that could arise by de novo mutation, mitotic recombination, or sequencing artifact. An allelic plot was generated and color-coded based on this estimation. N-J and RaxML trees were generated for each unphased sequenced marker using pairwise distance matrices as input.

WGS Methods. Libraries were prepared for 24 isolates (*SI Appendix*, Table S3) using the TruSeq DNA library kit and sequenced on an Illumina HiSeq X. Illumina paired-end reads were mapped to reference genomes available on TritrypDB (tritrypdb.org v.63), using the BWA-MEM aligner v0.7.17 with default parameters. Mean sequencing coverage of mapped reads was 35.2 (SD = 67.6), according to Qualimap v.2.2.1, and WGS reference mapping stats for each sample are provided (*SI Appendix*, Table S3). Sequence alignment map files were converted to binary alignment map (BAM) files and sorted by genomic position using samtools v1.10 (38). SNPs and chromosome copy numbers (somy) were determined using the PAINT software suite designed for studying inheritance patterns in aneuploid genomes (39). Sequence alignment files were used as input to PAINT to determine the list of alleles in each genomic position with a custom-built caller (39) using the *findReadDepth* and *findAlleles* utilities, respectively. Normalized allele frequencies were determined using PAINT *listAlleles*. SNPs were identified by comparing each sample to the reference genome using PAINT *findSNPs*. Merged files containing SNP frequencies from all samples mapped to the same reference genome were generated using PAINT *findAlleleFreqsSNPpositions*. SNPs were considered heterozygous if allele frequencies were between 0.4–0.6 and homozygous if ≥0.85 for each genomic position. Allele frequencies of <0.15, read depth <10, or represented by <25% of reads in either forward or reverse direction were filtered out of the analysis. SNPs were filtered according to frequency using a custom shell script, PAINT-generated merged frequency files and individual SNP format files. Positional allele frequency of filtered SNPs was visualized for selected chromosomes as scatter plots using the *ggplot2* (40) R package in RStudio v2023.3.0.386 (RStudio Team). To evaluate local heterozygosity and homozygosity ratios across the genome, PAINT SNP format files were converted to variant call format (v.4.3) and browser extensible data (BED) using a custom python script and BEDOPS *vcf2bed* v.2.4.41 (41), separately for homozygous (het) and heterozygous (hom) SNPs. Reference genomes were split into 10-kb regions with BEDOPS *--chop*, which were then used as reference for mapping each sample SNP BED file and counting heterozygous and homozygous SNPs using BEDOPS *bedmap*. Relative het/homo ratios within each 10-kb window were calculated by a custom shell script and used as input to Circos v.0.69 (42) to generate circos plots for data visualization, with conditional painting of genomic windows in red if het/homo ≥0.4 or blue otherwise. Chromosome somies were inferred by calculating the normalized median read depth multiplied by 2 (assuming a diploid genome) using the *ConcatenatedPloidyMatrix* utility with a 5-kb window size. Genomic regions of multiple sequence repeats and high copy number variation were filtered out from the analysis by eliminating positions with coverage levels ≥2-fold or ≤0.5-fold the average chromosome coverage. Somy values were rounded up to the second decimal point and visualized as heat maps using the *ComplexHeatmap* R package (43) in v2023.3.0.386 (RStudio Team).

Data, Materials, and Software Availability. The raw reads for samples generated in this study have been deposited in the NCBI database under BioProject PRJNA1395251 (44) and will remain publicly available without restriction. All study data are included in the article and/or *SI Appendix*.

ACKNOWLEDGMENTS. We thank Yves Balard, Patrick Lami, Laurence Lachaud, and Patrick Bastien for carefully reviewing *SI Appendix*, Table S1. The work in Tunisia was supported by a CRDF Grant (TN1-7009-TP09) and the Ministry of Higher Education and Scientific Research (LR11IPT04 and LR16IPT04). I.G. is supported by the DELTAS Africa II program, Wellcome and FCDO (DEL22-005). Further support by the Czech Grant Agency (Grant 23-06479X) and the Intramural Research Program of the NIH is acknowledged. The contributions of the NIH authors are considered Works of the United States Government. The findings and conclusions presented in this paper are those of the author(s) and do not necessarily reflect the views of the NIH or the US Department of Health and Human Services.

Author affiliations: [a]Molecular Parasitology Section, Laboratory of Parasitic Diseases, National Institute of Allergy and Infectious Diseases, National Institutes of Health, Bethesda, MD 20892; [b]Laboratory of Molecular Epidemiology and Experimental Pathology, Institut Pasteur de Tunis, and University of Tunis El Manar, Tunis 1002, Tunisia; [c]Intracellular Parasite Section, Laboratory of Parasitic Diseases, National Institute of Allergy and Infectious Diseases, National Institutes of Health, Bethesda, MD 20892; [d]Department of Biological Sciences, Mississippi State University, Starkville, MS 39762; [e]Department of Parasitology, Faculty of Sciences, Charles University, Prague 12800, Czechia; [f]Department of Parasitology, Faculty of Medicine, University of Sousse, Sousse 4000, Tunisia; [g]Institut Pasteur d'Algérie, Algiers 16047, Algeria; [h]Institute of Parasitology, Biology Centre, Czech Academy of Sciences, České Budějovice 37005, Czechia; and [i]Faculty of Science, University of South Bohemia, České Budějovice 37005, Czechia

Author contributions: I.G., J.L., and M.E.G. designed research; E.V.C.A.-F., M.B., M.W.B., Z.H., and M.E.G. performed research; M.B., P.V., Y.S.-B., I. Khammari, I. Kherachi, A.F.M., and J.L. contributed new reagents/analytic tools; E.V.C.A.-F., M.B., T.R.F., M.W.B., D.L.S., J.L., and M.E.G. analyzed data; and E.V.C.A.-F., M.W.B., D.L.S., J.L., and M.E.G. wrote the paper.

Reviewers: T.B., Julius-Maximilians-Universitat Wurzburg; and L.G., Istituto Superiore di Sanità, Rome.

1. P. Desjeux, Leishmaniasis: Current situation and new perspectives. *Comp. Immunol. Microbiol. Infect. Dis.* **27**, 305–318 (2004).
2. J. Alvar *et al.*, Leishmaniasis worldwide and global estimates of its incidence. *PLoS One* **7**, e35671 (2012).
3. D. M. Pigott *et al.*, Global distribution maps of the leishmaniases. *Elife* **3**, e02851 (2014).
4. J. Shaw, The leishmaniases–survival and expansion in a changing world. A mini-review. *Mem. Inst. Oswaldo Cruz* **102**, 541–547 (2007).

5. World Health Organization, Leishmaniasis (2023). https://www.who.int/news-room/fact-sheets/detail/leishmaniasis. Accessed 15 June 2025.
6. J. Heitman, Evolution of eukaryotic microbial pathogens via covert sexual reproduction. *Cell Host Microbe* **8**, 86–99 (2010).
7. M. E. Grigg, S. Bonnefoy, A. B. Hehl, Y. Suzuki, J. C. Boothroyd, Success and virulence in *Toxoplasma* as the result of sexual recombination between two distinct ancestries. *Science* **294**, 161–165 (2001).
8. J. P. Boyle *et al.*, Just one cross appears capable of dramatically altering the population biology of a eukaryotic pathogen like *Toxoplasma gondii*. *Proc. Natl. Acad. Sci. U.S.A.* **103**, 10514–10519 (2006).
9. M. Tibayrenc, F. J. Ayala, How clonal are *Trypanosoma* and *Leishmania*? *Trends Parasitol.* **29**, 264–269 (2013).
10. C. M. C. Catta-Preta, D. L. Sacks, Genetic exchange in *Leishmania*: Understanding the cryptic sexual cycle. *Annu. Rev. Microbiol.* **79**, 105–128 (2025).
11. M. B. Rogers *et al.*, Genomic confirmation of hybridisation and recent inbreeding in a vector-isolated Leishmania population. *PLoS Genet.* **10**, e1004092 (2014).
12. J. A. Cotton *et al.*, Genomic analysis of natural intra-specific hybrids among Ethiopian isolates of Leishmania donovani. *PLoS Negl. Trop. Dis.* **14**, e0007143 (2020).
13. P. Lypaczewski, G. Matlashewski, Leishmania donovani hybridisation and introgression in nature: A comparative genomic investigation. *Lancet Microbe* **2**, e250–e258 (2021).
14. N. S. Akopyants *et al.*, Demonstration of genetic exchange during cyclical development of *Leishmania* in the sand fly vector. *Science* **324**, 265–268 (2009).
15. V. Rougeron, T. De Meeus, S. Kako Ouraga, M. Hide, A. L. Banuls, "Everything you always wanted to know about sex (but were afraid to ask)" in *Leishmania* after two decades of laboratory and field analyses. *PLoS Pathog.* **6**, e1001004 (2010).
16. E. Inbar *et al.*, Whole genome sequencing of experimental hybrids supports meiosis-like sexual recombination in Leishmania. *PLoS Genet.* **15**, e1008042 (2019).
17. A. Romano *et al.*, Cross-species genetic exchange between visceral and cutaneous strains of *Leishmania* in the sand fly vector. *Proc. Natl. Acad. Sci. U.S.A.* **111**, 16808–16813 (2014).
18. M. Akhoundi *et al.*, Leishmania infections: Molecular targets and diagnosis. *Mol. Aspects Med.* **57**, 1–29 (2017).
19. M. Tibayrenc, F. Kjellberg, F. J. Ayala, A clonal theory of parasitic protozoa: The population structures of *Entamoeba*, *Giardia*, *Leishmania*, *Naegleria*, *Plasmodium*, *Trichomonas*, and *Trypanosoma* and their medical and taxonomical consequences. *Proc. Natl. Acad. Sci. U.S.A.* **87**, 2414–2418 (1990).
20. B. Bulle *et al.*, Practical approach for typing strains of *Leishmania infantum* by microsatellite analysis. *J. Clin. Microbiol.* **40**, 3391–3397 (2002).
21. W. Weir *et al.*, Population genomics reveals the origin and asexual evolution of human infective trypanosomes. *Elife* **5**, e11473 (2016).
22. K. Kuhls *et al.*, Differentiation and gene flow among European populations of Leishmania infantum MON-1. *PLoS Negl. Trop. Dis.* **2**, e261 (2008).
23. T. R. Ferreira *et al.*, Self-Hybridization in Leishmania major. *MBio* **13**, e0285822 (2022).
24. P. Volf *et al.*, Increased transmission potential of *Leishmania major*/*Leishmania infantum* hybrids. *Int. J. Parasitol.* **37**, 589–593 (2007).
25. J. Lukeš *et al.*, Evolutionary and geographical history of the *Leishmania donovani* complex with a revision of current taxonomy. *Proc. Natl. Acad. Sci. U.S.A.* **104**, 9375–9380 (2007).
26. T. R. Ferreira, At the genetic crossroads of Leishmania: Emerging hybrids reshaping disease patterns. *PLoS Pathog.* **21**, e1013213 (2025).
27. F. Bruno *et al.*, Genomic and epidemiological evidence for the emergence of a L. infantum/L. donovani hybrid with unusual epidemiology in northern Italy. *MBio* **15**, e0099524 (2024).
28. H. Imamura *et al.*, Evolutionary genomics of epidemic visceral leishmaniasis in the Indian subcontinent. *Elife* **5**, e12613 (2016).
29. F. Ariey *et al.*, A molecular marker of artemisinin-resistant *Plasmodium falciparum* malaria. *Nature* **505**, 50–55 (2014).
30. O. Miotto *et al.*, Multiple populations of artemisinin-resistant *Plasmodium falciparum* in Cambodia. *Nat. Genet.* **45**, 648–655 (2013).
31. S. Guerbouj, I. Guizani, S. De Doncker, J. C. Dujardin, N. Nuwayri-Salti, Identification of Lebanese dermotropic putative *Leishmania archibaldi* isolates by gp63 PCR-RFLP. *Trans. R. Soc. Trop. Med. Hyg.* **95**, 687–688 (2001).
32. S. Guerbouj *et al.*, Evaluation of a gp63-PCR based assay as a molecular diagnosis tool in canine leishmaniasis in Tunisia. *PLoS One* **9**, e105419 (2014).
33. G. Schonian *et al.*, PCR diagnosis and characterization of *Leishmania* in local and imported clinical samples. *Diagn. Microbiol. Infect. Dis.* **47**, 349–358 (2003).
34. B. Q. Minh *et al.*, IQ-tree 2: New models and efficient methods for phylogenetic inference in the genomic era. *Mol. Biol. Evol.* **37**, 1530–1534 (2020).
35. Z. Yang, PAML 4: Phylogenetic analysis by maximum likelihood. *Mol. Biol. Evol.* **24**, 1586–1591 (2007).
36. K. Tamura, G. Stecher, D. Peterson, A. Filipski, S. Kumar, MEGA6: Molecular evolutionary genetics analysis version 6.0. *Mol. Biol. Evol.* **30**, 2725–2729 (2013).
37. D. H. Huson, D. Bryant, Application of phylogenetic networks in evolutionary studies. *Mol. Biol. Evol.* **23**, 254–267 (2006).
38. P. Danecek *et al.*, Twelve years of SAMtools and BCFtools. *Gigascience* **10**, giab008 (2021).
39. J. S. Shaik, D. E. Dobson, D. L. Sacks, S. M. Beverley, Leishmania sexual reproductive strategies as resolved through computational methods designed for aneuploid genomes. *Genes* **12**, 167 (2021).
40. H. Wickham, *ggplot2: Elegant Graphics for Data Analysis* (Springer International Publishing, Springer Cham, 2016), 10.1007/978-3-319-24277-4.
41. S. Neph *et al.*, BEDOPS: High-performance genomic feature operations. *Bioinformatics* **28**, 1919–1920 (2012).
42. M. Krzywinski *et al.*, Circos: An information aesthetic for comparative genomics. *Genome Res.* **19**, 1639–1645 (2009).
43. Z. Gu, R. Eils, M. Schlesner, Complex heatmaps reveal patterns and correlations in multidimensional genomic data. *Bioinformatics* **32**, 2847–2849 (2016).
44. E. V. Alves-Ferreira *et al.*, Leishmania sp. raw sequence reads: WGS of 24 isolates. NCBI BioProject. https://www.ncbi.nlm.nih.gov/bioproject/PRJNA1395251. Accessed 1 April 2026.